Table III. Calculation of Bond Energy in Compounds of Heavier Transitional Elements

compd	$-\delta_X$	R_c, pm	R_o, pm	E_c, kcal	E_i, kcal	E(calcd), kcal	E(exptl), kcal	compd	$-\delta_X$	R_c, pm	R_o, pm	E_c, kcal	E_i, kcal	E(calcd), kcal	E(exptl), kcal
YF_3	0.466	254.9	204	4.6	151.5	156.1	155.3	$TaBr_5$	0.089	290.2	244.5	16.2	72.5	88.7	87.4
YCl_3	0.407	286.2	247	9.2	109.4	118.6	122.5	TaI_5	0.072	309.3	266	16.8	53.5	70.3	82.3
YBr_3	0.378	301.0	263	10.7	75.3	106.0	101.9	WF_6	0.150	241.1	182.9	24.7	95.3	120.0	121.7
YI_3	0.324	320.1	280	13.4	76.9	90.3	91.7	WCl_6	0.119	272.4	226	22.2	60.9	83.1	83.2
ZrF_2	0.627	250.7	192	4.2	162.7	166.9	159.2	WBr_6	0.103	287.2	240	21.8	49.7	71.5	70.2
$ZrCl_2$	0.556	282	230	8.7	120.3	129.0	122.9	WCl_5	0.157	272.4	226	20.1	69.4	89.5	89.5
$ZrBr_2$	0.519	296.8	247	10.3	104.7	115.0	120.3	WBr_5	0.139	287.2	240	19.9	57.5	77.4	77.4
ZrI_2	0.453	315.9	266	12.8	84.9	97.7	106.2	ZrO_2	0.453	252.8	171.1	24.4	131.9	156.3	166.5 ± 6
ZrF_3	0.424	250.7	193	10.6	145.8	156.4	155.6	MoO_3							
$ZrCl_3$	0.367	282	230	14.1	105.8	119.9	118.6	Mo=O″	0.145	244.4	180	61.8	79.6	141.4	140.7
$ZrBr_3$	0.338	296.8	239	15.6	93.8	109.4	109.5	WO_3							
ZrI_3	0.289	315.9	259	17.6	73.2	90.8	91.7	W=O″	0.217	243.2	181	34.8	118.4	153.2	150.7
ZrF_4	0.328	250.7	190.2	12.9	143.1	156.0	156.3	WOF_4							
$ZrCl_4$	0.280	282	232	15.6	100.3	115.9	117.3	W—F‴	0.190	241.1	183	25.1	93.8 (×4)	475.7	
$ZrBr_4$	0.258	298.8	247	16.5	86.8	103.3	102.8	W≡O‴	0.083	243.2	181	48.8	151.7	200.5	
ZrI_4	0.214	315.9	268	18.5	66.2	84.7	83.2							676.2	676.7 ± 6
NbF_5	0.202	246.5	188	28.1	107.2	135.3	136.5	$WOCl_4$							
$NbCl_5$	0.165	277.8	226.5	27.0	72.6	99.6	97.8	W—Cl‴	0.128	272.4	226	22.3	60.7 (×4)	331.9	
$NbBr_5$	0.146	292.6	245.5	26.2	59.2	85.4	82.4	W≡O‴	0.185	243.2	181	50.8	144.6	195.4	
MoF_6	0.105	242.3	182.5	46.4	66.5	112.9	112.8							527.3	515.7 × 5
$MoCl_6$	0.076	273.6	226	39.0	38.9	77.9	77.9	WO_2Cl_2							
HfF_4	0.348	248.1	190.9	7.2	151.1	158.3	155.7	W—Cl′	0.142	272.4	226	20.1	60.4 (×2)	161.0	
$HfCl_4$	0.299	279.4	233	10.1	106.6	116.7	119.0	W≡O‴	0.198	243.2	181	50.9	143.9 (×2)	389.5	
$TaCl_5$	0.099	275.4	230	15.8	85.5	101.3	102.8							550.5	540.7 ± 6

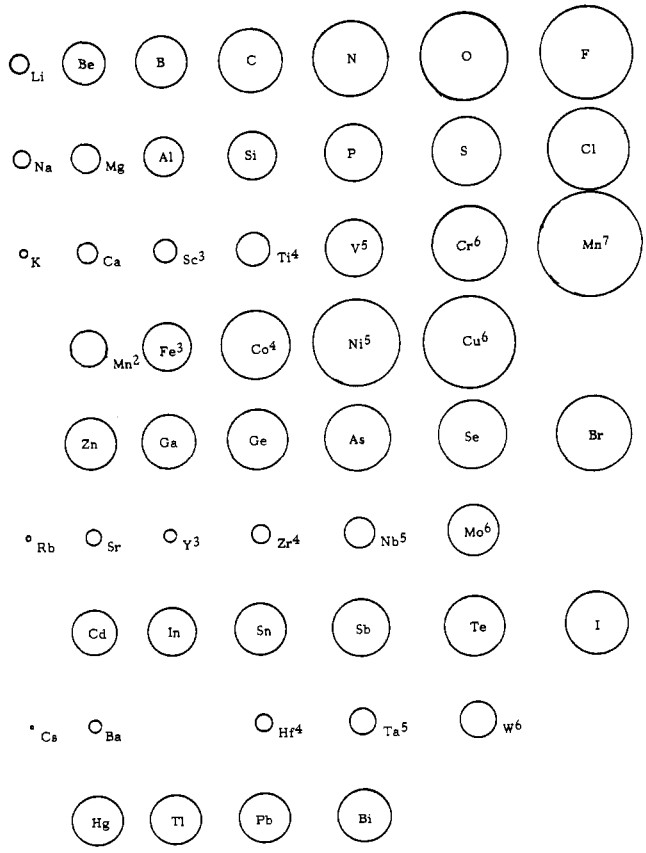

Figure 3. Relative electronegativities. (Superscript number is the oxidation number; this designation is suggested as more convenient than the usual Roman numerals in parentheses.)

copper all resemble the halogens in their electronegativity, but this is not true of the heavier elements of these transitional groups. The high values are of course estimates made from extensive extrapolation and are not to be considered accurate, but they do present a picture that is at least qualitatively correct.

No doubt the new electronegativity values will provide useful insights concerning the chemistry of transitional elements that will correspond to earlier results from application of partial charges and bond energies to major-group chemistry. They should also contribute to better understanding of the solid state that transitional elements exhibit in most of their compounds.

Registry No. Sc, 7440-20-2; Y, 7440-65-5; Ti, 7440-32-6; Zr, 7440-67-7; Hf, 7440-58-6; V, 7440-62-2; Nb, 7440-03-1; Ta, 7440-25-7; Cr, 7440-47-3; Mo, 7439-98-7; W, 7440-33-7; Mn, 7439-96-5; Fe, 7439-89-6; Co, 7440-48-4; Ni, 7440-02-0; Cu, 7440-50-8.

Contribution from the Department of Chemistry, Washington University, St. Louis, Missouri 63130

Pentadienyl–Metal–Phosphine Chemistry. 7.[1] Synthesis, Solid-State Structure, and Solution Dynamics of (η^5-Pentadienyl)tris(phosphine)rhenium Complexes. Measurement of the Rotational Barrier for the Pentadienyl Ligand

John R. Bleeke* and Dennis A. Moore

Received January 22, 1986

Electron-rich cyclopentadienyl–metal–phosphine complexes have recently attracted a great deal of interest because of their ability to activate bonds that are generally resistant to activation. For example, Bergman[2] has recently shown that (η^5-cp)Re(PMe_3)$_3$ will, upon photolysis, activate C–H bonds in methane, while Green[3] has demonstrated that (η^5-cp)Mn(PMe_3)$_3$ will activate C–O bonds in carbon dioxide.

We have initiated a systematic study of the chemistry of electron-rich metal–phosphine complexes containing the acyclic pentadienyl ligand (pd).[1,4] These complexes are expected to be even more electron-rich than their cyclopentadienyl analogues[5]

(1) For the previous paper in this series, see: Bleeke, J. R.; Stanley, G. G.; Kotyk, J. J. *Organometallics*, in press.
(2) Bergman, R. G.; Seidler, P. F.; Wenzel, T. T. *J. Am. Chem. Soc.* **1985**, *107*, 4358.
(3) Green, M. L. H.; Joyner, D. S.; Wallis, J.; Bell, J. P. Presented at the 190th National Meeting of the American Chemical Society, Chicago, IL, Sept 1985.
(4) (a) Bleeke, J. R.; Hays, M. K. *Organometallics* **1983**, *2*, 1263. (b) Bleeke, J. R.; Peng, W.-J. *Ibid.* **1984**, *3*, 1422. (c) Bleeke, J. R.; Kotyk, J. J. *Ibid.* **1985**, *4*, 194.

0020-1669/86/1325-3522$01.50/0

Table I. Positional Parameters with Estimated Standard Deviations for Non-Hydrogen Atoms in (η^5-2,4-Me_2pd)Re(PMe_2Ph)$_3$ (**2**)

atom	x	y	z	atom	x	y	z
Re	0.13610 (3)	0.18758 (7)	0.05826 (4)	C8P1	0.129 (1)	0.284 (2)	−0.261 (1)
P1	0.1591 (2)	0.3297 (6)	−0.0735 (3)	C1P2	0.221 (1)	0.259 (3)	0.258 (1)
P2	0.2169 (2)	0.2791 (5)	0.1320 (3)	C2P2	0.237 (1)	0.489 (2)	0.125 (2)
P3	0.0755 (2)	0.3664 (6)	0.1256 (3)	C3P2	0.2881 (8)	0.196 (2)	0.101 (1)
C1	0.106 (1)	0.033 (2)	0.174 (1)	C4P2	0.2915 (9)	0.083 (2)	0.036 (1)
C2	0.1515 (8)	−0.043 (2)	0.126 (1)	C5P2	0.344 (1)	0.025 (3)	0.009 (2)
C3	0.1491 (9)	−0.067 (2)	0.026 (1)	C6P2	0.392 (1)	0.084 (4)	0.054 (2)
C4	0.1108 (9)	−0.013 (2)	−0.033 (1)	C7P2	0.389 (1)	0.195 (5)	0.115 (2)
C5	0.0608 (9)	0.066 (2)	−0.003 (1)	C8P2	0.3355 (8)	0.248 (3)	0.145 (2)
C6	0.204 (1)	−0.106 (2)	0.178 (2)	C1P3	0.0032 (9)	0.307 (4)	0.128 (2)
C7	0.1207 (9)	−0.042 (3)	−0.133 (1)	C2P3	0.062 (1)	0.563 (3)	0.080 (2)
C1P1	0.2259 (9)	0.291 (3)	−0.126 (1)	C3P3	0.0872 (8)	0.418 (2)	0.247 (1)
C2P1	0.166 (1)	0.550 (3)	−0.072 (2)	C4P3	0.1123 (9)	0.562 (3)	0.270 (2)
C3P1	0.113 (1)	0.320 (4)	−0.176 (1)	C5P3	0.121 (1)	0.591 (4)	0.364 (2)
C4P1	0.056 (1)	0.378 (3)	−0.166 (2)	C6P3	0.102 (1)	0.487 (4)	0.433 (2)
C5P1	0.024 (1)	0.402 (4)	−0.239 (2)	C7P3	0.076 (1)	0.349 (3)	0.407 (2)
C6P1	0.042 (1)	0.356 (4)	−0.325 (2)	C8P3	0.0689 (8)	0.313 (3)	0.315 (1)
C7P1	0.097 (1)	0.297 (3)	−0.334 (1)				

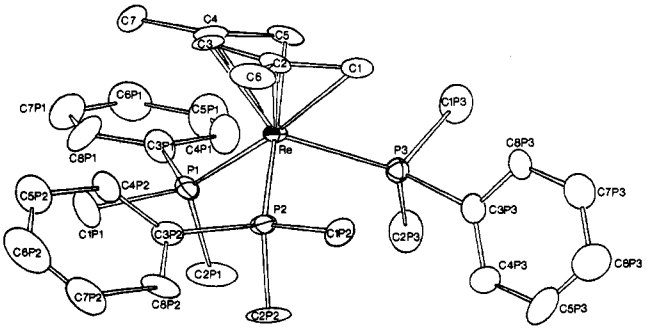

Figure 1. ORTEP drawing of (η^5-2,4-Me_2pd)Re(PMe_2Ph)$_3$ (**2**). Heavy atoms are represented by thermal ellipsoids drawn to encompass 25% of the electron density.

and have the added feature that they can create coordinative unsaturation by interconverting between relatively stable π-bonded η^5-pd and η^3-pd modes.[4] We anticipate that these features will, in general, impart unique reactivity to pd–M–phosphine complexes.

We now describe the syntheses, structures, and solution dynamics of two new η^5-pentadienyl–Re–tris(phosphine) complexes, (η^5-pd)Re(PMe_2Ph)$_3$ (**1**) and (η^5-2,4-Me_2pd)Re(PMe_2Ph)$_3$ (**2**). Variable-temperature NMR studies have enabled us to calculate pd ligand rotational barriers in these complexes. The reaction chemistry of these electron-rich complexes will be reported in a separate communication.

Results and Discussion

A. Syntheses of (η^5-pd)Re(PMe_2Ph)$_3$ (1) and (η^5-2,4-Me_2pd)Re(PMe_2Ph)$_3$ (2). (η^5-pd)Re(PMe_2Ph)$_3$ (**1**) and its 2,4-dimethylpentadienyl analogue **2** are produced in high yield from the reaction of *fac*-$ReCl_3(PMe_2Ph)_3$[6] with 4 or more equiv of the potassium salt of the appropriate pentadienide.[7] In this reaction, pentadienide serves as both the alkylating and reducing agent.[8] Preliminary studies indicate that a similar approach can be used to produce (η^5-pd)Re(PR_3)$_3$ complexes containing phosphines with a wide range of steric and electronic features.

B. Structure of (η^5-2,4-Me_2pd)Re(PMe_2Ph)$_3$ (2). An ORTEP drawing of **2** based on an X-ray structural analysis is presented in Figure 1. Atomic coordinates for the non-hydrogen atoms are listed in Table I. Important bond distances and angles are reported in Table II. The complex assumes an approximate octahedral geometry with C1, C3, and C5 of the pd ligand and

Table II. Selected Bond Distances (Å) and Bond Angles (deg) with Estimated Standard Deviations for (η^5-2,4-Me_2pd)Re(PMe_2Ph)$_3$ (**2**)

Bond Distances

Re–P1	2.364 (4)	Re–C3	2.28 (1)	C3–C4	1.35 (3)
Re–P2	2.350 (5)	Re–C4	2.28 (2)	C4–C5	1.44 (3)
Re–P3	2.343 (5)	Re–C5	2.27 (2)	C2–C6	1.57 (3)
Re–C1	2.29 (2)	C1–C2	1.46 (3)	C4–C7	1.52 (3)
Re–C2	2.27 (2)	C2–C3	1.49 (3)		

Bond Angles

P1–Re–P2	90.6 (2)	P2–Re–C3	108.2 (5)	C3–Re–C5	64.8 (8)
P1–Re–P3	98.2 (2)	P2–Re–C5	171.7 (5)	C1–C2–C3	121 (2)
P2–Re–P3	94.9 (2)	P3–Re–C1	83.2 (5)	C2–C3–C4	129 (2)
P1–Re–C1	172.5 (6)	P3–Re–C3	144.6 (6)	C3–C4–C5	122 (2)
P1–Re–C3	107.9 (5)	P3–Re–C5	89.5 (6)	C6–C2–C1	122 (2)
P1–Re–C5	95.8 (5)	C1–Re–C3	68.0 (6)	C7–C4–C5	120 (2)
P2–Re–C1	96.7 (5)	C1–Re–C5	76.8 (7)		

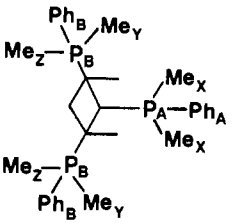

Figure 2. Labeling scheme for phosphine ligands in (η^5-pd)Re(PMe_2Ph)$_3$, showing chemically inequivalent phosphorus atoms, phenyl groups, and methyl groups.

P1, P2, and P3 of the phosphine ligands occupying the six coordination sites.

The five metal-bound carbon atoms of the 2,4-dimethylpentadienyl ligand are coplanar to within 0.03 Å, while the pd methyl carbon atoms are bent substantially out of the pd plane toward the Re atom (0.076 and 0.068 Å).[9] Phosphorus atom P3 is bent up into the mouth of the pd ligand; i.e., P3 is 2.24 Å from the pd plane while P1 and P2 are 3.23 and 3.20 Å away, respectively.[10]

The phenyl rings on the PMe_2Ph ligands are arranged in a fanlike orientation. The phenyl ring on the mouth phosphorus atom (P3) is almost perpendicular to the pd ligand (dihedral angle = 87.5°), while the phenyl rings on P2 and P1 make dihedral angles of 43.6 and 8.2° with the pd plane, respectively.

C. Solution Dynamics. Compounds **1** and **2** are fluxional as a result of relatively low barriers to rotation of the pd or 2,4-Me_2pd group with respect to the Re(PMe_2Ph)$_3$ fragment. Stopped-ex-

(5) (a) Cotton, F. A. *Chemical Applications of Group Theory*; Wiley-Interscience: New York, 1971. (b) Ernst, R. D. *Acc. Chem. Res.* **1985**, *18*, 56.
(6) Douglas, P. G.; Shaw, B. L. *Inorg. Synth.* **1977**, *17*, 64.
(7) Yasuda, H.; Ohnuma, Y.; Yamauchi, M.; Tani, H.; Nakamura, A. *Bull. Chem. Soc. Jpn.* **1979**, *52*, 2036.
(8) A similar approach has proved successful in the Mn and Co systems.[1,4b,c]
(9) This is a common feature of (η^5-2,4-Me_2pd)M complexes. It probably results from the atomic p_z orbitals on C2 and C4 bending toward the metal atom to achieve better overlap with the appropriate metal orbitals.
(10) We have made similar observations in the structures of (η^5-pd)MnP_3 complexes (see ref 1).

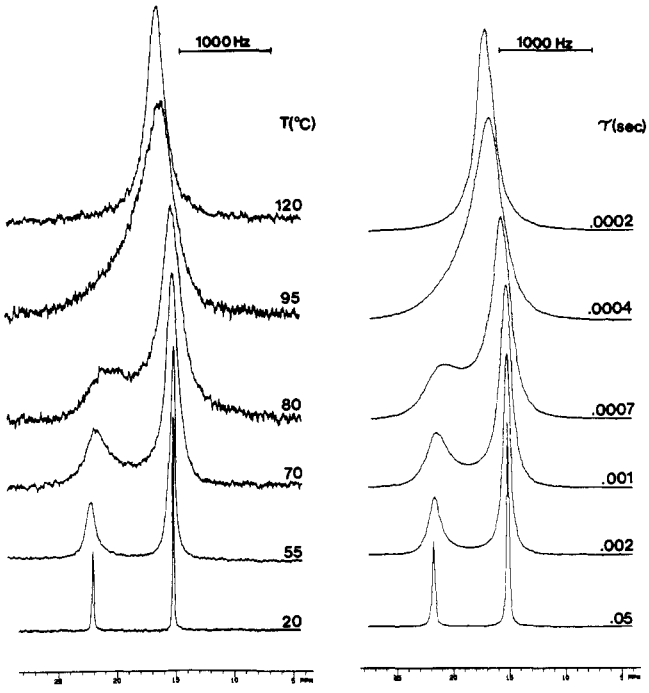

Figure 3. Left: Variable-temperature $^{31}P\{^1H\}$ NMR spectra of $(\eta^5$-pd)$Re(PMe_2Ph)_3$ (**1**). Right: Calculated ^{31}P NMR line shapes with preexchange lifetimes τ (in s) between successive pd ligand rotations. Note that $1/\tau = k_{total} = 2k_{clockwise} = 2k_{counterclockwise}$, where $k_{clockwise}$ and $k_{counterclockwise}$ are the rates of clockwise and counterclockwise pd ligand rotation, respectively.

Table III. $\Delta G^{\ddagger}$ Values for Pentadienyl Ligand Rotation in Compounds **1** and **2**

compd	nucleus	exchanging atoms	temp range,[a] °C	$\Delta G^{\ddagger}$, kcal/mol
1	^1H	phosphine methyl hydrogens	20–105	16.6 ± 0.3
1	^{31}P	phosphine phosphorus atoms	20–105	16.3 ± 0.2
2	^1H	phosphine methyl hydrogens	−45–80	13.9 ± 0.3
2	^{13}C	ortho carbons of phenyls	−60–50	13.4 ± 0.2

[a] Temperature range over which $\Delta G^{\ddagger}$ was calculated.

change NMR spectra are observed at 22 °C for **1** and −65 °C for **2**. Two types of chemically inequivalent phosphorus nuclei (P_A and P_B in Figure 2) are observed in the stopped-exchange ^{31}P NMR spectra, two types of inequivalent phenyl groups (Ph_A and Ph_B; Figure 2) are observed by ^{13}C and ^1H NMR spectroscopy, and three types of inequivalent phosphine methyl groups (Me_x, Me_y, and Me_z; Figure 2) are seen in the ^1H and ^{13}C NMR spectra. As the temperature is raised, the rate of pd or 2,4-Me_2pd ligand rotation increases, exchanging P_A with P_B, exchanging Ph_A with Ph_B, and exchanging Me_x, Me_y, and Me_z.[11]

Line shape simulations of the variable-temperature ^{31}P NMR spectra (see Figure 3), the methyl region of the ^1H NMR spectra, and the phenyl ortho region of the ^{13}C spectra[12] have enabled us to calculate a $\Delta G^{\ddagger}$ of 16.4 kcal/mol for rotation of the pd ligand in **1** and a $\Delta G^{\ddagger}$ of 13.7 kcal/mol for rotation of the 2,4-Me_2pd ligand in **2**.[13] As can be seen from Table III, the calculated $\Delta G^{\ddagger}$'s are self-consistent and do not depend on the nucleus observed. Furthermore, $\Delta G^{\ddagger}$ does not have a significant temperature dependence, indicating that $\Delta S^{\ddagger}$ for the fluxional process is small.

(11) Pentadienyl ligand ^{13}C and ^1H NMR signals are unaffected by the exchange.
(12) These are relatively uncluttered regions of the spectra. Furthermore, the line shapes of the peaks in these regions are suitable for simulation.
(13) Phosphine methyl group exchange, phosphine phenyl group exchange, and exchange of P_A with P_B can occur by either a 120° clockwise rotation *or* a 120° counterclockwise rotation of the pd ligand. Hence, the total rate of exchange, k_{total}, is equal to the sum of the rates of exchange due to clockwise rotation and counterclockwise rotation ($k_{total} = 2k_{clockwise} = 2k_{counterclockwise}$). $\Delta G^{\ddagger}$'s are calculated by using $k_{clockwise}$ *or* $k_{counterclockwise}$.

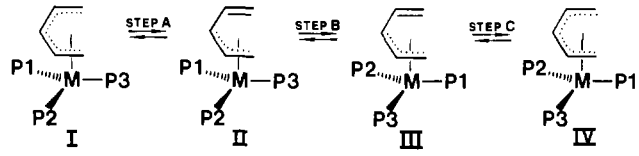

Figure 4. Mechanism II for rotation of pentadienyl ligand with respect to $Re(PMe_2Ph)_3$ fragment, involving (a) $\eta^5 \rightarrow \eta^3$ pd ligand isomerization, (b) rotation of η^3-pd ligand, and (c) reisomerization back to η^5 bonding mode.

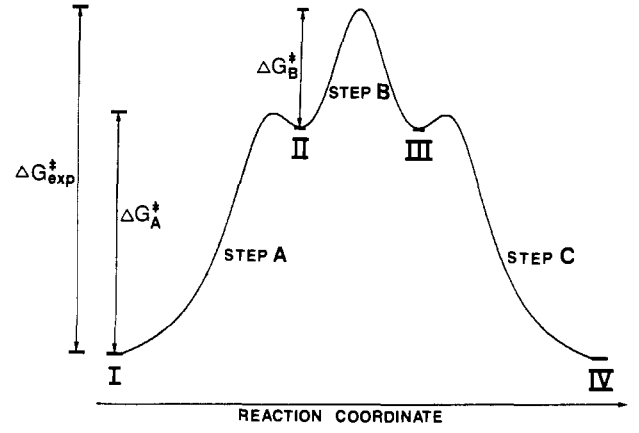

Figure 5. Idealized graph of free energy vs. reaction coordinate for pentadienyl ligand rotation, mechanism II. Steps a–c and species I–IV are described in Figure 4.

This is consistent with an intramolecular ligand rotation process.

D. Mechanism of Pentadienyl Ligand Rotation. Two plausible mechanisms for the pd ligand rotation can be proposed. The first is a simple rotation of the ligand in the η^5-bonding mode. The second mechanism involves three steps: (a) an initial isomerization to an η^3-mode (I → II; Figure 4), (b) rotation of the η^3-pd ligand (II → III; Figure 4), and (c) reisomerization of the ligand back to an η^5-mode (III → IV; Figure 4). In the second mechanism, steps a and b will both be accompanied by substantial free energies of activation. The overall measured $\Delta G^{\ddagger}_{exptl}$ for the ligand rotation process will be approximately equal to the sum of the $\Delta G^{\ddagger}$'s for steps a and b (see Figure 5), assuming that II is close to the transition state for the $\eta^5 \rightarrow \eta^3$ pd isomerization process.

Although at this point we cannot rule out mechanism I, mechanism II nicely accounts for the observed relationships between $\Delta G^{\ddagger}_{exptl}$ and ligand electronics. In Mechanism II, the magnitude of $\Delta G^{\ddagger}_a$ should decrease as the electron-donating ability of the ligands increases, since good electron-donating ligands can more effectively stabilize the 16-e η^3-pd intermediate, II. Therefore, assuming that $\Delta G^{\ddagger}_b$ is relatively independent of electronic effects, mechanism II predicts an overall inverse relationship between the magnitude of $\Delta G^{\ddagger}_{exptl}$ and electron-donating ability of the ligands. This relationship is, in fact, observed. Compound **2**, which possesses the better electron-donating ligand, 2,4-dimethylpentadienyl, has a lower $\Delta G^{\ddagger}_{exptl}$ than compound **1**, which possesses the less effective donor ligand, pentadienyl.[14]

Rotational barriers for η^3-allyl ligands are typically about 5 kcal/mol,[15] and this is probably a good estimate for $\Delta G^{\ddagger}_b$. Subtracting 5 kcal/mol from our experimentally determined values of $\Delta G^{\ddagger}$ ($\Delta G^{\ddagger}_{exptl}$), we obtain values for $\Delta G^{\ddagger}_a$ of 11.4 and 8.7 kcal/mol for **1** and **2**, respectively.

Experimental Section

A. General Comments. All manipulations were carried out under inert atmosphere by using either drybox or Schlenk techniques. Tetrahydrofuran was dried with sodium/benzophenone and distilled before use. Pentane was dried over calcium hydride and distilled. Dimethyl-

(14) We have also observed an inverse relationship between $\Delta G^{\ddagger}_{exptl}$ and the electron-donating ability of the ligands for a series of (pd)Mn–tris(phosphine) complexes (see ref 1).
(15) Mingos, D. M. P. In *Comprehensive Organometallic Chemistry*; Pergamon: Oxford, England, 1982; Vol. 3, pp 60–67.

phenylphosphine was obtained from Strem Chemicals; pentadiene and 2,4-dimethylpentadiene were purchased from Wiley Organics. All were used without further purification. All NMR experiments were performed on a Varian XL-300 NMR spectrometer. ^1H (300-MHz) and ^{13}C (75-MHz) spectra are referenced to tetramethylsilane. ^{31}P (121-MHz) spectra are referenced to external H_3PO_4.[16] In general, ^{13}C NMR peak assignments were made from gated decoupled spectra. ^1H NMR peak assignments were then obtained from ^{13}C–^1H shift-correlated (HETCOR) 2D spectra. In some cases, connectivities were ascertained from ^1H–^1H shift-correlated (COSY) 2D spectra. Infrared spectra were recorded on a Perkin-Elmer 283B spectrophotometer. Low-resolution mass spectra were obtained on a Finnigan 3200 GC/MS. High-resolution mass spectra were obtained with a VG-ZAB-3F mass spectrometer operated in the double-focusing mode, at a mass resolution of 7000, and data were processed by using an associated VG-11-250 data system. Microanalyses were performed by Galbraith Laboratories, Inc., Knoxville, TN.

B. Synthesis of (η^5-pd)Re(PMe_2Ph)$_3$ (1). A solution containing 2.0 g (1.1×10^{-2} mol) of KC_5H_7·THF[7] in 100 mL of tetrahydrofuran (THF) was added dropwise to a cold (−78 °C) stirred solution of 2.0 g (2.8×10^{-3} mol) of *fac*-$ReCl_3(PMe_2Ph)_3$[6] in 30 mL of THF. When the addition was complete (approximately 40 min), the reaction mixture was allowed to warm to room temperature and stirred for an additional 2–3 h. At this time, the solvent was removed in vacuo. The resulting dark red residue was extracted with pentane, slurried with charcoal, and filtered through a Celite pad on a coarse glass frit. The resulting bright yellow solution was then concentrated and cooled to −30 °C to effect crystallization; the yield of yellow crystalline product was 1.3 g (69.5%).

The following data are from stopped-exchange spectra. Refer to Figure 2 for phosphine labeling scheme. ^1H NMR (20 °C, benzene-d_6): δ −0.24 ($H1_{anti}$, 2 H, dd, J_{H-H2} = 8.8 Hz, $J_{H-H1_{syn}}$ = 2.2 Hz), 1.31 (Me_y or M_z, 6 H, s), 1.39 (Me_y or Me_z, 6 H, s), 1.95 (Me_x, 6 H, d, J_{H-P} = 6.3 Hz), 2.10 ($H1_{syn}$, 2 H, dd, J_{H-H2} = 7.8 Hz, $J_{H-H1_{anti}}$ = 2.2 Hz), 4.41 (H2, 2 H, br m), 5.04 (H3, 1 H, t, J_{H-H2} = 5.1 Hz), 7.16–7.51 (phenyl H's, 15 H, m). $^{13}C\{^1H\}$ NMR (20 °C, benzene-d_6): δ 21.31 (Me), 24.30 (Me), 26.06 (Me), 37.68 (C1/C5), 81.99 (C3), 85.44 (C2/C4), 127.0–130.0 (phenyl C's). $^{31}P\{^1H\}$ (20 °C, benzene-d_6): δ −32.51 (P_B, 2 P), −25.75 (P_A, 1 P). IR (22 °C, benzene): 3017–2908 cm^{-1} (s, C–H stretches); 1471, 1432, 1288, 1273 cm^{-1} (s, C–C and P–C stretches); 930, 893 cm^{-1} (vs, P–C stretches). MS (low resolution, electron impact, solid probe, 70 eV): M^+ at 666 and 668. MS (high resolution, electron impact, solid probe, 70 eV): calcd for M^+, 666.187, 668.190; found, 666.188, 668.194. Anal. Calcd for $ReP_3C_{29}H_{40}$: C, 52.15; H, 6.05. Found: C, 52.29; H, 6.04.

C. Synthesis of (η^5-2,4-Me_2pd)Re(PMe_2Ph)$_3$ (2). The same procedure as above was followed, except that the KC_5H_7·THF reagent was replaced with 2.3 g (1.1×10^{-2} mol) of KC_7H_{11}·THF;[7] the yield of yellow-orange crystalline product was 1.1 g (56.4%). The following data are from stopped-exchange spectra. Refer to Figure 2 for phosphine labeling scheme. ^1H NMR (−45 °C, toluene-d_8): δ −0.10 ($H1_{anti}$, 2 H, br s), 1.32 (Me_y or Me_z, 6 H, br s), 1.44 (Me_y or Me_z, 6 H, br s), 1.77 (pd Me, 6 H, s), 1.84 (Me_x, 6 H, d, J_{P-H} = 6.6 Hz), 1.90 ($H1_{syn}$, 2 H, br s), 5.12 (H3, 1 H, s), 6.95–7.39 (phenyl H's, 15 H, complex m). $^{13}C\{^1H\}$ (−60 °C, toluene-d_8): δ 24.90–25.65 (Me_y and Me_z, complex m), 25.93 (pd Me, s), 28.58 (Me_x, d, J_{C-P} = 24.1 Hz), 41.85 (C1/C5, br s), 83.57 (C3, s), 96.25 (C2/C4, s), 127.12–128.75 (para and meta carbons of phenyl rings, complex m, partially obscured by solvent peaks), 129.83 (ortho carbons of Ph_A, d, J_{C-P} = 5.1 Hz), 131.94 (ortho carbons of Ph_B, d, J_{C-P} = 7.9 Hz), 144.91 (ipso-C of P_B, d, J_{C-P} = 30.0 Hz), 149.06 (ipso-C of P_A, d, J_{C-P} = 37.1 Hz). $^{31}P\{^1H\}$ NMR (−65 °C, toluene-d_8): δ −28.55 (P_B, 2 P), −28.07 (P_A, 1 P). IR (22 °C, benzene): 3010–2902 cm^{-1} (s, C–H stretches); 1468, 1430, 1284, 1270 cm^{-1} (s, C–C and P–C stretches); 925, 890 cm^{-1} (vs, P–C stretches). MS (low resolution, electron impact, solid probe, 70 eV): M^+ at 694 and 696. Anal. Calcd for $ReP_3C_{31}H_{44}$: C, 53.50; H, 6.39. Found: C, 51.65; H, 6.28.

D. X-ray Diffraction Study of 2. Single crystals suitable for X-ray diffraction were grown from a saturated pentane solution. Data were collected at room temperature on a Nicolet P3 diffractometer, using graphite-monochromated Mo Kα radiation. A very fast scan rate (6–29° min^{-1}) was employed, because the crystal decayed in the X-ray beam. A linear decay correction was applied to the data, but an absorption correction was not performed. All data reduction and structure refinement were carried out by using the Enraf-Nonius structure determination package (modified by B. A. Frenz and Associates, Inc., College Station, TX) on a VAX 11/780 computer. Crystal data and details of data collection and structure analysis are summarized in Table IV. Further details are provided in the supplementary material. This structure determination establishes the connectivity of the atoms; no detailed analysis of bond distances or angles is warranted at this level of precision.

Table IV. Crystal and Diffraction Data for Compound **2**

formula	$ReP_3C_{31}H_{44}$
fw	695.82
space group[a]	$P2_12_12_1$
a, Å	23.83 (1)
b, Å	8.705 (3)
c, Å	14.715 (6)
V, Å^3	3053 (4)
Z	4
cryst color	yellow-orange
cryst dimens, mm	0.6 × 0.5 × 0.4
d_{calcd}, g/cm^3	1.514
radiation	Mo Kα, λ = 0.71069 Å
μ_{calcd}, cm^{-1}	42.06
abs cor	none
scan type	ω
scan rate, deg/min	variable, 6–29
scan width, deg	0.6
2θ min, deg	3
2θ max, deg	55
octant collcd	$+h,+k,+l$
no. of reflcns measd	3346
no. of reflcns with $I > 3\sigma(I)$	2488
decay of stds	26.7%
min, max, and av decay cor applied to f_{obsd}	1.00009, 1.17134, 1.07713
no. of params varied	316
data/param ratio	7.873
final R_F[b]	0.056
final R_{wF}[c]	0.068

[a] Uniquely determined from systematic absences: $h00$, $h = 2n + 1$; $0k0$, $k = 2n + 1$; $00l$, $l = 2n + 1$. [b] $R_F = \sum||F_o| - |F_c||/\sum|F_o|$. [c] $R_{wF} = [\sum w(|F_o| - |F_c|)^2/\sum w|F_o|^2]^{1/2}$; $w = 1/\sigma(|F_o|)$.

E. Solution Dynamics of Compounds 1 and 2. Samples were dissolved in toluene-d_8 or *o*-xylene-d_{10}, and NMR spectra were recorded over the temperature range −75 to 135 °C. Probe temperatures were calibrated by using the temperature dependence of the difference in chemical shift between the ^1H resonances of the methyl and hydroxyl groups of methanol below ambient temperatures and between the ^1H resonances of the methylene and hydroxyl groups of ethylene glycol above ambient temperatures.[17] Theoretical lineshapes were calculated for a series of rates using the method of Johnson.[18,19] The experimental spectra (measured at various temperatures) were matched against the theoretical spectra, and in this way, exchange rate constants were determined for each temperature. These exchange rate constants, k, were then used to calculate the free energy of activation, ΔG^*, at each temperature, T, by using the Eyring equation: $k = (k'/h)Te^{-\Delta G^*/RT}$.[20]

Conclusion

Electron-rich η^5-pentadienyl–Re(PR_3)$_3$ complexes can be synthesized in high yield by reacting *fac*-$ReCl_3(PR_3)_3$ with excess potassium pentadienide. In the solid state, these complexes exhibit the expected octahedral geometry, with one phosphine ligand residing under the "mouth" of the pd group and the other two lying beneath the "backbone". In solution, the molecules are fluxional as a result of relatively low barriers of pd group rotation. The dependence of the rotational barriers on the electron-donating ability of the pd ligand suggests that the mechanism for the rotation involves (a) an $\eta^5 \rightarrow \eta^3$ pd ligand isomerization, (b) rotation of the η^3-bound ligand, and (c) reisomerization back to the η^5-bonding mode. The reactivity of these electron-rich molecules is currently under investigation in our laboratories.

(16) The ^{31}P NMR signal for free dimethylphenylphosphine lies 47.55 ppm upfield from that for free H_3PO_4.

(17) Von Geet, A. L. *Anal. Chem.* **1968**, *40*, 2227.
(18) Johnson, C. S., Jr. *Am. J. Phys.* **1967**, *35*, 929.
(19) Martin, M. L.; Martin, G. J.; Delpuech, J.-J. *Practical NMR Spectroscopy*; Heydon: London, 1980; pp 303–309.
(20) Lowry, T. H.; Richardson, K. S. *Mechanism and Theory in Organic Chemistry*; Harper and Row: New York, 1976.

Acknowledgment. We thank the donors of the Petroleum Research Fund, administered by the American Chemical Society, for financial support. Additional support was provided by Monsanto Co. and by Grant No. S07 RR07054-20 awarded by the Biomedical Research Support Grant Program, Division of Research Resources, National Institutes of Health. NMR spectra were obtained with the expert assistance of Dr. Andre d'Avignon, director of the Washington University High Resolution NMR Service Facility. This facility was funded in part by NIH Biomedical Research Support Instrument Grant 1 S10 RR02004 and by a gift from Monsanto Co. We thank Dr. Andrew Tyler of Washington University Medical School and Dr. M. Grayson of McDonnell Douglas, Inc., Berkeley, MO, for obtaining mass spectra of **1** and **2**. Finally, we thank Professor G. G. Stanley (Washington University) and David J. Rauscher for assistance with the single-crystal X-ray diffraction study of **2**.

Registry No. **1**, 103712-54-5; **2**, 103712-55-6; KC_5H_7·THF, 51197-67-2; *fac*-$ReCl_3(PMe_2Ph)_3$, 24627-46-1; KC_7H_{11}·THF, 103712-56-7.

Supplementary Material Available: Detailed description of X-ray diffraction data collection, data reduction, and structure refinement and listings of final atomic coordinates, thermal parameters, bond lengths, bond angles, and significant least-squares planes including subtended dihedral angles (10 pages); a listing of observed and calculated structure factor amplitudes (10 pages). Ordering information is given on any current masthead page.

Contribution from the Department of Chemistry and Laboratory for Molecular Structure and Bonding, Texas A&M University, College Station, Texas 77843, and Departamento de Quimica Inorganica, Facultad de Quimica, Universidad de Valencia, Burjasot, Valencia, Spain

Preparation of Iridium(III) Complexes Containing the Phosphine P(*o*-BrC_6F_4)(Ph)$_2$. A New Example of η^2-Coordination and Halocarbon Binding in an (*o*-Haloaryl)phosphine

F. Albert Cotton,*† Pascual Lahuerta,*‡ Mercedes Sanau,‡ Willi Schwotzer,† and Isabel Solana‡

Received February 12, 1986

It has recently been observed that (*o*-haloaryl)phosphines can act as bidentate ligands coordinating via the phosphorus and a halogen atom. Examples of such behavior have been encountered in rhodium[1,2] and iridium[3] complexes.

Rhodium(I) compounds containing the title ligand (abbreviated PCBr) can undergo thermal orthometalation by metal insertion into the C-Br bond. In general, mononuclear products are isolated that contain a four-membered metallocycle.[4] There is, however, one example of an orthometalated phosphine bridging a dirhodium(4+) unit, produced in a 2c-2e oxidative addition reaction.[2]

In probing the reactivity of PCBr in complexes of Ir, we now find that the reaction of $IrCl_3$·xH_2O in refluxing ethanol does not yield metalated species. Instead, a mononuclear complex, $IrCl_3(PCBr)_2$ (**1**), is isolated in high yield. The ^{31}P NMR spectrum shows two different P environments. Subsequent reaction with PPh_3 leads to the replacement of one of the PCBr ligands to yield $IrCl_3(PCBr)(PPh_3)$ (**2**). It is an octahedral complex with an unusual bonding mode of the PCBr ligand.

Experimental Section

PCBr was prepared by published procedures.[5] All solvents were dried and purified by standard procedures. All reactions were carried out in an atmosphere of dry dinitrogen.

Preparation of $IrCl_3(PCBr)_2$. Weighed amounts of 75 mg (0.21 mmol) of $IrCl_3$·xH_2O and 352 mg (0.84 mmol) of PCBr were refluxed in 10 mL of EtOH (96%) for 2 h. The resulting yellow solution was cooled to room temperature, and a cream colored product was obtained upon vacuum concentration. It was filtered off, washed with hexane, and recrystallized from a CH_2Cl_2/hexane mixture. Yield: 70%. Anal. Calcd for $C_{36}H_{20}F_8Cl_3Br_2P_2Ir$: C, 38.4; H, 1.6; Cl, 9.6. Found: C, 38.4; H, 1.6; Cl, 9.5. IR: C-F stretches at 1000-1100 cm^{-1}. $^{31}P\{^1H\}$ NMR: δ = 18.6, -14.4 (relative H_3PO_4); $^2J_{PP}$ = 509 Hz.

Preparation of $IrCl_3(PCBr)(PPh_3)$ (2). $IrCl_3(PCBr)_2$ (112 mg, 0.1 mmol) and 26 mg (0.1 mmol) of PPh_3 were dissolved in 5 mL of $CHCl_3$. The solution was stirred until all of the starting material had reacted as monitored by TLC. After addition of hexane and vacuum evaporation of part of the solvent a light colored product precipitated. It was collected by filtration, washed with hexane, and recrystallized from CH_2Cl_2/hexane. Crystals suitable for X-ray analysis were grown by slow diffusion of hexane into a CH_2Cl_2 solution. Yield: 85%. Anal. Calcd for $C_{36}H_{25}F_4Cl_3BrP_2Ir$: C, 43.4; H, 2.5. Found: C, 42.8; H, 2.4. $^{31}P\{^1H\}$ NMR: δ = 11.7, -20.6 $^2J_{PP}$ = 492 Hz.

X-ray Procedures. A yellow crystal of approximate dimensions 0.2 × 0.1 × 0.08 mm^3 was mounted on the tip of a glass fiber. All geometrical and intensity data were gathered from this crystal. Preliminary cell parameters were derived from 15 centered reflections and confirmed, together with the monoclinic symmetry, by axial photographs.

The systematic absences uniquely determined the space group $P2_1/n$. The data were corrected for Lorentz and polarization effects before structure factors were derived.[6] A semiempirical absorption correction was based on nine azimuthal scans at Eulerian angle χ close to 90°.

The position of the Ir center was derived from a three-dimensional Patterson map. The remaining non-hydrogen atoms were located and refined by alternating difference Fourier maps and least-squares cycles.

Table I. Crystal Data for $IrCl_3(PCBr)(PPh_3)$ (**2**)

formula	$IrCl_3P_2F_4BrC_{36}H_{25}$
fw	974.01
space group	$P2_1/n$
syst absences	$h0l$, $h + l = 2n$; $0k0$, $k = 2n$
a, Å	12.723 (7)
b, Å	15.066 (8)
c, Å	18.939 (9)
α, deg	90.0
β, deg	108.14 (2)
γ, deg	90.0
V, Å^3	3450 (6)
Z	4
d_{calcd}, g/cm^3	1.875
cryst size, mm	0.2 × 0.1 × 0.08
μ(Mo Kα), cm^{-1}	53.758
data collcn instrum	Syntex P$\bar{1}$
radiation (monochromated in incident beam)	Mo Kα ($\lambda_{\bar{\alpha}}$ = 0.71073 Å)
orientation reflcns: no., range (2θ)	15, 16-28
temp, °C	25
scan method	ω-2θ
data collcn range 2θ, deg	4.5-50
no. of unique data, total with $F_o^2 > 3\sigma(F_o^2)$	2550, 2391
no. of params refined	244
transmissn factors: max, min	1.0, 0.69
R^a	0.0544
R_w^b	0.0675
quality-of-fit indicator^c	1.347
largest shift/esd, final cycle	1.75
largest peak, e/Å^3	0.7

$^a R = \sum||F_o| - |F_c||/\sum|F_o|$. $^b R_w = [\sum w(|F_o| - |F_c|)^2/\sum w|F_o|^2]^{1/2}$; $w = 1/\sigma^2(|F_o|)$. ^{c} Quality-of-fit = $[\sum w(|F_o| - |F_c|)^2/(N_{observns} - N_{params})]^{1/2}$.

(1) Solans, X.; Font-Altaba, M.; Aguilo, M.; Miratvilles, C.; Besteiro, J. C.; Lahuerta, P. *Acta Crystallogr. Sect. C: Cryst. Struct. Commun.* **1985**, *C41*, 841.
(2) Barcello, F. L.; Lahuerta, P.; Ubeda, M. A.; Foces-Foces, C.; Cano, F. H.; Martinez Ripoll, M. *J. Chem. Soc., Chem. Commun.* **1985**, 43.
(3) Burk, M. J.; Crabtree, R. H.; Holt, E. M. *Organometallics* **1984**, *3*, 638.
(4) Barcelo, F. L.; Besteiro, J. C.; Lahuerta, P.; Foces-Foces, C.; Cano, F. H.; Martinez Ripoll, M. *J. Organomet. Chem.* **1984**, *270*, 343.
(5) Eller, P. G.; Meek, D. W. *J. Organomet. Chem.* **1979**, *22*, 631.
(6) The Enraf-Nonius Structure Determination Package (SDP Plus) was used for all crystallographic computation.

† Texas A&M University.
‡ Universidad de Valencia.

